THESIS FOR THE DEGREE OF DOCTOR OF PHILOSOPHY

Drift Waves in General Toroidal Equilibria

Johan Anderson

Submitted to the School of Electrical Engineering,
Chalmers University of Technology
in partial fulfillment of the requirements for the degree of
Doctor of Philosophy

Department of Electromagnetics
Chalmers University of technology
Göteborg, April 2002

Drift Waves in General Toroidal Equilibria
Johan E Anderson
ISBN:91-7291-138-7
Doktorsavhandlingar vid Chalmers Tekniska Högskola
ISSN:0346-718X
Nr i serien 1820

Technical Report No. 426
Department of Electromagnetics
Chalmers University of Technology
S-41296 Göteborg
Sweden
Telephone + 46 (0)31 - 7721000

Printed by Bibliotekets Reproavdelning
Göteborg, Sweden 2002

Drift Waves in General Toroidal Equilibria
Johan Anderson
Department of Electromagnetics
Chalmers University of Technology

Abstract

One of the main concerns in fusion research is to understand the anomalously high transport in magnetically confined plasmas. In recent years, substantial progress in the understanding of transport in terms of drift waves in fusion plasmas has been achieved. It is at present an important issue to investigate the stability of drift waves in realistic toroidal geometries.

Among the drift wave candidates for explaining the anomalous transport are the toroidal η_i-modes ($\eta_i = L_n/L_{T_i}$ or ITG driven modes) in the core and the resistive η_i-modes and the resistive ballooning modes in the edge.

The effects of plasma shaping on magneto-hydrodynamic (MHD) modes have been thoroughly studied. However, the effects of plasma shaping on the drift waves are not well known. Empirically it is found that the overall effects of elongation on the energy confinement time is favorable with $\tau_E \propto \kappa^{0.5}$.

In this thesis, the η_i-mode and the resistive edge mode stability in a non-circular tokamak geometry are studied. In particular, the effects of elongation and Shafranov shift are studied. In the core plasma a destabilization of the η_i-mode with increasing elongation is found whereas a stabilization is found in the edge region (or rather for peaked density profiles).

Moreover, a comparison of the η_i growth rates in the tokamak and stellarator equilibria is made. The growth rates for the tokamak and stellarator cases are comparable whereas the modulus of the real frequency is substantially larger in the stellarator. In addition, a stronger stabilization of the ITG mode growth is found for large $\epsilon_n (= L_n/R)$ in the stellarator case.

Finally, an analytical estimation of zonal flow generation including effects of elongation is presented. The results suggest that a strong excitation of zonal flows is obtained for peaked density profiles and close to marginal stability..

However, in order draw more detailed conclusions of the effects of elongation on the global confinement time, a more extensive study

using predictive transport simulations, which treats the edge and core transport processes self-consistently will be needed.

Descriptors: fusion plasmas, drift waves, instabilities, toroidal geometry

Listing of papers

The Phd thesis is based on the work presented in the following papers

Paper A

Thermal transport in collision dominated edge plasmas
R. Singh, H. Nordman, J. Anderson and J. Weiland
Physics of Plasmas **5**, 3669 (1998)

Paper B

Effects of non-circular tokamak geometry on ion-temperature-gradient driven modes
J. Anderson, H. Nordman, J. Weiland
Plasma Physics and Controlled Fusion **42**, 545 (2000)

Paper C

Effects of cross-sectional elongation on the resistive edge modes
J. Anderson, H. Nordman, J. Weiland
Physics of Plasmas **8**, 180 (2001)

Paper D

Ion-temperature-gradient modes in stellarator geometry
T. Rafiq, J. Anderson, M. Nadeem, M. Persson
Plasma Physics and Controlled Fusion **43**, 1363 (2001)

Paper E

A comparison of drift wave stability in tokamak and stellarator geometry
J. Anderson, T. Rafiq, M. Nadeem, M. Persson

Physics of Plasmas **9** (2002)

Paper F

Zonal flow generation in ion-temperature-gradient mode turbulence
J. Anderson, H. Nordman, R. Singh, J. Weiland
Submitted to Physics of Plasmas

Contents

To Melissa

I Introduction

In the near future the world total energy demand will increase tremendously as the population will grow and the developing countries become more industrialized. At the 1997 Kyoto climate conference, it was agreed that the world wide emission of the green house gases should be reduced to only 5 percent above the 1990 figures in the near future. If these conditions are to be met, additional energy sources friendly to the environment are needed. This need will be further increased since the traditional energy sources, oil and other fossil fuels[1], will soon become much more scarce and obviously more expensive. The viable alternatives are the renewables[2] and the nuclear energy sources.

Nuclear fusion is nowadays among the probable sources of energy for the centuries to come. The fusion reactions of interest in a future reactor are

$$D + D \rightarrow He^3 + n + 3.27MeV \quad (1)$$

$$D + D \rightarrow T + H + 4.05MeV \quad (2)$$

$$D + T \rightarrow He^4 + n + 17.58MeV \quad (3)$$

where D is deuterium, He is helium, n is a neutron, T is tritium and H is hydrogen. The first two reactions are of almost equal probability.

From an environmental point of view, the $D-D$ reactions are preferable, since deuterium is stable and is available in nature as one part in 6700 of the hydrogen in sea water. The deuterium in one liter of sea water could contribute with as much energy as approximately 300 liters of gasoline. Tritium on the other hand is not generally found in nature since its half life is 12.4 years and it thus must be manufactured or bred in the reactor. However, the $D-D$ reactions are much more difficult to obtain than the $D-T$ reactions and need a higher burning temperature.[3]

In this thesis only thermonuclear fusion is considered. Then thermal energy is to be distributed among the reacting particles allowing them to overcome the Coulomb barrier and the inevitable losses. It is sufficient if only a few percent of the particles participate in the reactions, since the energy released in each reaction is large.

[1] Coal may be an exception to this but coal has a more deep negative impact on the environment than the others.

[2] Solar, wind and biomass

[3] Around 100 keV in $D-D$ operation compared to 10 keV in $D-T$ operation.

In thermonuclear fusion it is convenient to confine the plasma[4] by a magnetic field. The condition of ignition for a fusion plasma is often expressed in the triple product as

$$nT_i\tau_E \geq 5 \cdot 10^{21} m^{-3} keVs \tag{4}$$

where n is the particle density, T_i is the ion temperature and τ_E is the energy confinement time.

The uncharged particles are not confined in the magnetic field and will eventually hit the vessel wall. This makes a possible source of tritium fuel, since the inside of the vessel wall may be covered with a lithium blanket that together with the high energy neutrons will produce tritium:

$$Li^6 + n \rightarrow T + He^4 + 4.8MeV \tag{5}$$
$$Li^7 + n \rightarrow T + He^4 + n - 2.5MeV. \tag{6}$$

To be able to confine the particles along the magnetic field it is preferable to have closed magnetic field lines, usually bent into a torus. The geometry of the magnetic flux surfaces are determined by balancing the magnetic pressure and the plasma pressure (more often recognized as the Grad-Shafranov equation in the 2-dim case).

It is important to note that the magnetically confined plasma is not in thermodynamic equilibrium. Hence there are a many sources of free energy that can drive instabilities. The sources of free energy (∇n, ∇T etc) may cause unstable modes (modes with growth $\gamma \geq 0$) that can destroy the equilibrium and result in a plasma disruption or turbulence that cause transport phenomena.

The instabilities are often divided into macroscopic (stability) and microscopic (transport) instabilities. The instabilities associated with macroscopic stability problems are called magneto-hydrodynamic (MHD) instabilities [1]; they may cause severe plasma disruptions on a very short time scale ($10^{-6}s$).

One of the most important issues in present fusion research is to understand transport in tokamaks [2] - [3], since there is a large discrepancy between the experimentally measured and the predicted neoclassical diffusion coefficients. The neoclassical transport theory [4] - [6] predicts that

[4]The term plasma comes from the Greek word $\pi\lambda\alpha\sigma\mu\alpha$ which means something like molded or fabricated. The term plasma was introduced into physics to describe the positive column in a glow discharge tube, by Langmuir 1928.

the diffusion coefficient drops as the temperature increases to values of thermonuclear fusion

$$D \propto \epsilon^{-3/2} q^2 \rho_L^2 \nu \propto \rho_L^2 \nu \propto T^{-1/2} \tag{7}$$

where ρ_L is the Larmor radius, ν is the collision frequency, q is the safety factor, $\epsilon = r/R$ where r is the minor radius and R is the major radius. However, it is found that in the direction perpendicular to the magnetic field lines the neoclassical theory fails to give good estimates

$$\frac{\chi_i^{exp}}{\chi_i^{neo}} \sim 3 - 10 \tag{8}$$

$$\frac{\chi_e^{exp}}{\chi_e^{neo}} \sim 10^2 \tag{9}$$

$$\frac{D_e^{exp}}{D_e^{neo}} \sim 10^2 \tag{10}$$

where χ_i is the ion heat diffusivity, χ_e is the electron heat diffusivity and D_e is the particle diffusivity.

The unexpectedly large transport observed in experiments and the theoretically predicted χ_j^{neo} $(j = i, e)$ and D_e^{neo} is referred to as the anomalous, i.e. non classical transport.

The dominant transport mechanism in tokamak plasmas seems to be due to the $\vec{E} \times \vec{B}$ convection although the possibility of transport due to magnetic perturbations cannot be ruled out [7]. Since temperature and density perturbations in general may be independent, $\vec{E} \times \vec{B}$ convection can lead to both conductive ($\propto \nabla T$) and convective ($\propto \nabla n$) energy transport.

The fluctuating fields are assumed to originate from micro instabilities in the plasma. The instabilities are driven by the free energy released because the magnetically confined plasma is most often not in thermodynamic equilibrium. As these instabilities grow they produce micro-turbulence with large electrical fields that tend to cause convective transport and if the electric field is random this becomes a usual diffusive process. In order to understand anomalous transport we need to estimate the diffusion coefficients.

A renormalization procedure gives [8], $\gamma = \gamma_{linear} - k^2 D$ (k is the wave number), where an integration over the diffusive particle orbits is performed. The system will reach a state were the non-linearities have saturated the total growth, giving $D = \gamma_{linear}/k^2$. Another way to achieve an estimate

of the saturation level, is to balance the linear growth with the dominant non-linear term, employing the equation

$$\frac{\partial n}{\partial t} \approx \vec{v}_E \cdot \nabla n \tag{11}$$

and setting $\frac{\partial}{\partial t} \rightarrow \gamma$ we obtain $\gamma = \vec{v}_E \cdot \vec{k}$ or $\frac{e\phi}{T_e} = \frac{\gamma}{\omega_\star} \frac{1}{k_x L_n}$. This leads to

$$D = \frac{\gamma^3/k^2}{\omega_r^2 + \gamma^2} \tag{12}$$

which reduces to $D \approx \gamma/k^2$ for strong turbulence [9] - [12]. The modes with small values of the eigenfrequency ω_r tend to contribute with the largest transport. The modes with high real frequency tend to mainly make the particles oscillate. This last result (Eq. 12) may also be derived from the non-Markovian Fokker-Planck equation [13]. From these estimations it is clear that it is of great importance to find means of suppressing the linear growth rates. The estimated anomalous diffusion coefficients have a temperature dependency completely different from the classical diffusion coefficients, with

$$D \propto \frac{\gamma}{k_\perp^2} \propto \frac{\omega_\star}{k_\perp^2} \propto \frac{\rho_L^2 c_s}{L_n} \frac{1}{k_\perp \rho_L} \propto T^{3/2} \tag{13}$$

where $\omega_\star$ is the drift frequency, c_s is the sound speed and L_n is the density scale length. It is assumed that the turbulent correlation length scales with the gyro-radius (Gyro-Bohm scaling) in order to take $k_\perp \rho_L$ as a free parameter.

The anomalous transport coefficients in general depend on the dynamic variables and their gradients. A typical property is that the transport coefficients increase with the gradients up to a certain limit after which they decrease with the gradient.

There are situations where the pressure gradient rapidly increases in certain zones compared to the surrounding regions, leading to a large reduction in the transport coefficient[5] within the region with increased pressure gradient [14] - [15]. This is an indication that the turbulence induced transport is reduced. It is here natural to use the term transport barrier.[6] Even if the

[5]The transport coefficient may even be decreased to the neoclassical level.

[6]C.f. H-mode. [19]

barrier width is only a few percent of the minor radius the energy confinement time may be increased by a factor of two or more.

The stabilization of turbulence may be the origin of transport barrier formation. Among the stabilizing mechanisms proposed are high and low magnetic shear[7] [14], [16] - [18] and velocity shear.[8]

The rest of this introduction is meant to clarify and explain some concepts and methods used in the Papers A to F. In Sec. 2 the ion-temperature-gradient driven modes and the resistive edge modes are discussed; in addition some properties of the ballooning mode formalism are reviewed. Sec. 3 contains a discussion of the analytical equilibrium model and geometry used in Papers A to C and F. In Sec. 4 the stellarator configuration and some differences between stellarators and tokamaks are discussed. Sec. 5 is dedicated to the concept of zonal flows and some of the consequences and the analytical methods for studying and estimating zonal flow excitation. In Sec. 6 a short summary of all appended papers is presented.

[7]High magnetic shear tends to stabilize certain modes while low magnetic shear tends to reduce the curvature drive and to separate the neighboring rational surfaces hence reducing the mode coupling effects.

[8]Velocity shear may tear turbulent eddies apart resulting in a reduction in their size and correlation length.

II The ion-temperature-gradient driven modes and the resistive edge modes

Drift waves are low frequency phenomena with short wavelengths and the drift wave ordering is defined through

$$k_{\parallel} v_{ti} << \omega_{\star} \sim \omega << k_{\parallel} v_{te} \tag{14}$$

and

$$k_{\perp} \rho \leq 1. \tag{15}$$

There are two main ways to model drift waves, either by kinetic theory or by fluid theory. Intermediate to these are the advanced fluid models that are derived from the kinetic models. In kinetic theory a plasma is described by the distribution function $f_j\left(t, \vec{r}, \vec{v}\right)$ (j refers to the particle species), representing the particle density in phase space $(\vec{r}, \vec{v})$. The time evolution is governed by the Boltzmann or Vlasov equations. In thermal equilibrium the velocity distribution is Maxwellian and if the distribution function is only allowed to change due to collisions the distribution function will approach a Maxwellian, regardless of the initial conditions and the collision term. For certain purposes it may not always be necessary to retain the detailed description of kinetic theory and we may instead use the macroscopic fluid description.

Only the advanced fluid models will be considered in this thesis. The fluid models are widely used since they are relatively simple to handle analytically and numerically as compared with the kinetic models. The main reason why the advanced fluid models are needed is that non-linear gyro-kinetic simulations still too time consuming to be run at transport time scale. Thus we need advanced fluid models to be able to run transport codes with first principles transport models. In different regions or in different parameter regimes of a tokamak plasma discharge, different physical phenomena become important. Hence it is important to identify the relevant physical phenomena in each region of interest.

Predictive transport code implementations [20] - [22] of the Chalmers drift wave model has been successful in reproducing experimental results such as the DIII-D electron heat pinch [23], the JET dimensionless scaling experiments [22], [24] and JET high performance discharges [25].

In this work I will concentrate on two different classes of modes; the first class is the ion-temperature-gradient (ITG) driven modes or η_i-modes [26] - [37] ($\eta_i = L_n/L_{T_i}$) (See Papers B, C, D, E and F) and the second class is the resistive edge modes (resistive η_i-mode and resistive ballooning mode, See Papers A and C) [37] - [42] since these modes are two of the main candidates for explaining the anomalous transport in the tokamak core and the edge region, respectively.

The ITG driven instability was first studied in the slab model as a modified ion acoustic wave [26]. In Ref. [27] this work was extended to nonuniform equilibrium density and retaining effects of magnetic shear while taking into account of ion kinetic effects. The toroidal branch of the η_i-mode was first investigated in [28] using the fluid description and the correct threshold for onset of instability in η_i was first found in [29] using kinetic theory. The toroidal η_i-mode is a Rayleigh-Taylor type of instability localized in the bad curvature region of the tokamak (the outside of the tokamak). It has a length scale intermediate between the MHD modes and the usual drift waves.

The edge fluctuations in present fusion plasmas are known to be large and are also related to the anomalous transport [30]. Many modes have been studied in order to explain these fluctuations. In Ref. [38] the resistive edge modes were investigated, in particular the resistive ballooning mode was shown to be a robust instability and thus it appeared reasonable that this mode can explain the growth of transport coefficients with minor radius in the edge region where η_i-modes and trapped electron modes cannot [39].

Since the magnetic field only confines particles in the perpendicular plane, the system is bent into a torus to take care of the third dimension. Toroidal effects are thus very fundamental. The toroidicity tends to localize the modes in the bad curvature region of the tokamak. These modes are called Ballooning modes. The localization in the bad curvature region imposes a finite $k_\parallel$ which, however still fulfills $k_\parallel << k_\perp$. The toroidal effects give a coupling between modes with different poloidal mode number m thus m is no longer a good "quantum number". The ballooning modes have been studied earlier in MHD [43] - [45].

For high mode number n, the long parallel wavelength and the short perpendicular wavelength decouples. However, this is in conflict with the periodicity requirement. When the mode number n is high, modes at different rational surfaces overlap and radially extended modes develop.

Using the ballooning mode formalism a general form of the eigenvalue equation which applies to several different types of modes is derived

$$\frac{\partial^2 \Psi}{\partial \chi^2} + f(\chi)\,\Psi = 0 \tag{16}$$

where Ψ is a generalized potential and χ is a generalized variable. For ballooning modes χ is the extended poloidal coordinate and in slab geometry χ is a Cartesian variable. The explicit form and interpretation of $f(\chi)$ in this equation varies with the type of mode considered. In the slab geometry $k_\parallel$ is just a number (may be function of $\vec{x}$) whereas in the ballooning representation it is an operator. Furthermore, for ballooning modes this operator is the source of the second derivative in Eq. 16. The original physical problem is now reduced to solving the eigenvalue equation Eq. 16, which is very similar to solving the problem of a particle in a potential well in quantum mechanics. If the potential $f(\chi)$ is formed in a well the modes are able to grow whereas if the potential is formed as an anti well the free energy that drives the instabilities disperse out and no modes can grow.

The acquired solutions (which are not the physical solutions) are not in general periodic but the physical solution and 2π-periodicity requirement could be recovered from a super position of the quasi-mode solutions. It can now be shown that the transformed problem gives the same eigenvalues as the original problem.

The eigenvalue problem in general has to be solved using numerical methods. One of the most widely used is the shooting technique were some boundary values are set (e.g. $\Psi(0) = 1, \Psi'(0) = 0$) and iterated until the condition $\Psi(\chi) \to 0$ as $\chi \to \infty$ is obtained. In the strong ballooning limit the eigenfunctions are well localized and the small χ approximation is valid. It is found that $f(\chi) \approx \tilde{A} - \tilde{B}\chi^2$ ($\mathtt{Re}\,\tilde{B}^{1/2} > 1$ for well localized modes) and the eigenvalue equation becomes the well known Weber equation with the solutions

$$\Psi_n = H_n\left(\chi \tilde{B}^{1/4}\right) e^{-\frac{1}{2}\tilde{B}^{1/2}\chi^2} \tag{17}$$

where H_n is the nth order Hermite polynomial. In this study, only the even modes are considered, since the even modes are expected to be more important for tokamak confinement than the odd modes.

In the expression of the mode growth it is observed that there is a threshold η_i value for onset of instability (p. 132 in [37]). Using a 2d model the growth rate can be written as

$$\gamma = \frac{\omega_\star \sqrt{\epsilon_n/\tau}}{1+k^2\rho^2}\sqrt{\eta_i - \eta_{ith}} \tag{18}$$

where $\epsilon_n = 2L_n/L_B$ and L_n, L_B are the density, magnetic field scale length, respectively. The remaining parameters are $\tau = T_i/T_e$ and the finite Larmor radius (FLR) parameter $k^2\rho^2 \approx 0.1$ for the fastest growing mode. It is found that the stability threshold is

$$\eta_{ith} \approx 2.72 L_n/L_B \tag{19}$$

for large ϵ_n, $\tau = 1$ and $k^2\rho^2 \to 0$. This stability condition can be written

$$L_{T_i} \geq 0.367 L_B \tag{20}$$

which is in good agreement with the kinetic result $L_{T_i} \geq 0.35 L_B$.

The ability to recover the stable regime of η_i-modes for large ϵ_n can conveniently be taken as a definition of an advanced fluid model [37].

In Papers A and C the resistive edge modes are investigated. In the core, the plasma is often assumed to be collisionless whereas at the edge the collisionless modes are not able to describe the continued growth of the transport coefficients with minor radius. At the edge the electrons are influenced by collisions whereas effects of trapping seem not to be important. This suggests that the resistive modes are an important source of the turbulence. The role of the resistive edge modes in the $(L-H)$ confinement phase transition has been thoroughly studied in recent years.

The two fluid model used in this thesis for the resistive ballooning mode (RBM) consists of the reduced Braghinskii equations for the electrons and an advanced fluid model for the ions. In the derived eigenmode equation, it is found that the spectrum of the resistive instability is very broad.

A way to visualize the RBM is to neglect the temperature effects in the electrostatic limit. Then in Eqs. 1 and 2 of Paper C it is found in a convenient normalization that

$$\nu J_\parallel = ik_\parallel (n-\phi) \tag{21}$$

$$\omega k_\perp^2 = k_\parallel J_\parallel - \omega_D n \tag{22}$$

where n is the ion density, ϕ is the electrostatic potential, $J_\parallel$ is the parallel current density, ν is the collisionality, $k_\parallel$, $k_\perp$ are the parallel and perpendicular length scales respectively and ω_D is the magnetic drift frequency. This leads to a phase shift relation relation for n and ϕ

$$n = \frac{k_\parallel^2 - i\nu\omega k_\perp^2}{k_\parallel^2 + i\nu\omega_D}\phi \tag{23}$$

Here the term in the numerator multiplied by ν is producing the collisional drift wave instability by causing a lagging phase shift between n and ϕ. This disturbance is driven by the background density gradient. If the curvature is unfavorable (e.g. on the outside of the tokamak) then the ω_D term in the denominator also tends to produce a destabilizing phase shift. The maximum value of ω_D is found at the outside midplane of the toroidal tokamak configuration and the mode "balloons" at this location.

In the large collisionality limit the RBM growth is weakly depending on the collisionality and asymptotically attains an ideal MHD type of response[9] $\gamma_0 = (2c_s^2/RL_n)^{1/2}$. This is a result of the limit $\nu_{ei} \to \infty$ ($D_{\parallel e} = 0$) in Eq. 15a in Paper A, retaining the ideal interchange mode dispersion relation modified by finite effects of η_i and ϵ_n.

For short wavelengths an analytical approximation in Eq. 15a in Paper A, leads to

$$\tilde{\gamma}^3 \propto (2s+1)\,\tilde{\nu}_{ei} \tag{24}$$

where s is the magnetic shear and ν_{ei} is the electron-ion collision frequency. This is the usual resistive ballooning mode and the growth rate is proportional to $\nu_{ei}^{1/3}$.

Using the same analytical approximation for long wavelengths it is found that the growth rate of the RBM is proportional to the collision frequency ($\gamma \propto \nu_{ei}$) [38].

[9]The collisionality is so large that it prevents the electrons from moving along the field lines.

III The tokamak equilibrium and geometry

An important problem that arises when investigating the effects of different magnetic field geometries on drift waves is the choice of equilibrium model. In most fusion reactors of interest we assume that the magnetic field lines lie in nested toroidal flux surfaces; this is not at all certain in 3d stellarators. The flux surfaces are toroidal surfaces with constant pressure, $\vec{B} \cdot \nabla P = 0$.

There are two kind of flux surfaces: (1) those where we have closed magnetic field lines (rational surface) and (2) those where the field lines are dense in the flux surface (ergodic surface). Before considering parameter regimes where drift waves are important we have to make sure that the plasma is MHD stable. This means that an equilibrium described by the stationary MHD equations $\vec{J} \times \vec{B} = \nabla p$, $\nabla \times \vec{B} = \vec{J}$ and $\nabla \cdot \vec{B} = 0$ must be stable against MHD perturbations. The first of these three equations describes pressure balance and the other are two of Maxwell's equations. In the tokamak case it is most often assumed that we have a two dimensional azimuthally symmetric configuration and the pressure balance is described by the Grad-Shafranov equation

$$\Delta^\star \psi = -R^2 \frac{dp}{d\psi} - F \frac{dF}{d\psi} \tag{25}$$

where $\Delta^\star = h_\xi^2 \nabla \cdot h_\xi^{-2} \nabla$, ξ is the "toroidal coordinate", $h_\xi = |\frac{\partial \vec{r}}{\partial \xi}|$, ψ is the flux surface label, F is associated with the current and p is the pressure whereas in the stellarator case we have to solve the full 3d problem. The Grad-Shafranov equation could either be solved numerically or by analytical approximations. A problem using the numerically computed equilibria is that it may be difficult to keep some parameters constant while varying others. On the other hand analytically computed equilibria are almost always based on expansions in inverse aspect ratio $\epsilon = a/R$ which may be quite large.

The analytically computed equilibrium, however, allows for controlled variation of the parameters that specify the equilibrium without recomputing it; this means, that it provides a model for investigating incorporated physical effects to the drift wave models.

A well known and widely used analytical equilibrium is the generalized $s-\alpha$ equilibrium [46] - [49] where it is possible to characterize approximated local equilibria using nine parameters; s (global magnetic shear), α (pressure gradient), A (aspect ratio), κ (elongation), δ (triangularity), q (safety factor),

and the variation of κ, δ and R with the flux surface. The computed equilibria are supposed to be stable for large enough time scales compared to the time scale of the drift waves. In paper [49], a quantitative agreement between numerical and analytical equilibria was found. Moreover, in a recent paper it was shown that the η_i-mode growth rate obtained with the analytical and the numerical equilibrium were in qualitative agreement [50] using a restriction to the equilibrium model used in [49].

Effects of plasma shaping has been studied thoroughly on the MHD modes; however, it is not at all well known how the properties of the drift waves change with plasma shaping. In particular, empirically it is found that elongation has a favorable effect on the energy confinement time $\tau_E \propto \kappa^{0.5}$ [51]. However, in recent preliminary studies strong and opposing effects of elongation on heat diffusivities in L-mode and H-mode, respectively, were found [52]. The effects of plasma shaping on drift wave stability has been studied before for the η_i-mode [53] - [55] and for the trapped electron mode [56] - [57].

In the physical model a change in the magnetic field geometry enter through the parallel and perpendicular mode numbers and the magnetic drift frequency, $k_\parallel$, $k_\perp$ and ω_D respectively. In modeling the magnetic flux surfaces it is common to use the Riemann metric tensor g_{ij} [58] - [59] defined as

$$\begin{aligned} ds^2 &= g_{rr}dr^2 + g_{\theta\theta}d\theta^2 + 2g_{r\theta}drd\theta + g_{\phi\phi}d\phi^2 \\ &= g_{ij}dx^i dx^j \end{aligned} \tag{26}$$

where $g_{rr}, g_{\theta\theta}, g_{r\theta}, g_{\phi\phi}$ are the relevant components of the metric tensor that defines the geometry. The inverse of the metric tensor is easily obtained from the relation $g_{ij}g^{jk} = \delta_i^k$, where δ_i^k is the Kronecker delta

$$g^{rr} = \frac{g_{\theta\theta}}{g_{rr}g_{\theta\theta} - g_{r\theta}^2} \tag{27}$$

$$g^{\theta\theta} = \frac{g_{rr}}{g_{rr}g_{\theta\theta} - g_{r\theta}^2} \tag{28}$$

$$g^{r\theta} = g^{\theta r} = -\frac{g_{r\theta}}{g_{rr}g_{\theta\theta} - g_{r\theta}^2}. \tag{29}$$

We would now like to calculate $\omega_D \propto \vec{k}\cdot e_\parallel \times \left(e_\parallel \cdot \nabla\right) e_\parallel$, defining $e_\parallel = \frac{\vec{B}}{B}$ and the B-field as $\vec{B} = B_\theta\hat{\theta} + B_\phi\hat{\phi}$. Defining ∇ as

$$\nabla = \nabla r\partial_r + \nabla\theta\partial_\theta + \nabla\phi\partial_\phi \tag{30}$$

we obtain the parallel derivative (this is also the parallel structure operator $k_\| = e_\| \cdot \nabla$)

$$e_\| \cdot \nabla = \frac{B_\phi}{B h_\phi}\partial_\phi + \frac{B_\theta}{B h_\theta}\partial_\theta. \tag{31}$$

Observe that there is no ϕ-dependence in any of the quantities $g_{\theta\theta}, g_{\phi\phi}$ or in B_θ, B_ϕ. This allows us to obtain

$$\begin{aligned}\left(e_\| \cdot \nabla\right) e_\| &= \frac{1}{B^2}\left(\frac{B_\phi^2}{h_\phi^2}\Gamma^j_{\phi\phi}e_j + \frac{B_\theta B_\phi}{h_\theta}\left(\partial_\theta h_\theta^{-1}e_\theta + h_\theta^{-1}\Gamma^j_{\theta\theta}e_j + \partial_\theta h_\phi^{-1}e_\phi\right.\right.\\ &+ \left.\left.\left(h_\theta^{-1}+h_\phi^{-1}\right)\Gamma^j_{\theta\phi}e_j\right) + \frac{B_\theta}{h_\theta^2}\partial_\theta B_\theta e_\theta + \frac{B_\theta}{h_\theta h_\phi}\partial_\theta B_\phi e_\phi\right)\\ &+ \| \, terms. \end{aligned} \tag{32}$$

Here we have used the fact that $\Gamma^j_{\theta\phi} = \Gamma^j_{\phi\theta} = 0$, $(j = r, \theta)$ neglecting the terms that are parallel to B because they will vanish when the cross product is calculated

$$\begin{aligned} e_\| \times \left(e_\| \cdot \nabla\right) e_\| &= \frac{J}{B^3}\left(\frac{B_\phi^3}{h_\phi^3}\left(e^\theta\Gamma^r_{\phi\phi} - e^r\Gamma^\theta_{\phi\phi}\right)\right.\\ &+ \frac{B_\theta B_\phi^2}{h_\theta^2 h_\phi}\left(e^\theta\Gamma^r_{\theta\theta} - e^r\Gamma^\theta_{\theta\theta}\right)\\ &- \frac{B_\theta B_\phi^2}{h_\theta h_\phi}\left(\partial_\theta h_\theta^{-1}e^r + h_\phi^{-1}e^\phi\Gamma^r_{\phi\phi}\right)\\ &+ \frac{B_\theta^2 B_\phi}{h_\theta^2 h_\phi}\left(e^\theta\Gamma^r_{\theta\theta} - e^r\Gamma^\theta_{\theta\theta}\right)\\ &+ \frac{B_\theta B_\phi}{h_\theta h_\phi}\left(h_\phi^{-1}e^r B_\theta\Gamma^\phi_{\theta\phi} - h_\theta^{-1}\partial_\theta B_\theta e^r\right)\\ &+ \left.\frac{B_\theta^2}{h_\theta^2}\left(-h_\theta^{-1}B_\phi\Gamma^r_{\phi\phi}e^\phi + h_\phi^{-1}\partial_\theta B_\phi e^r\right)\right). \end{aligned} \tag{33}$$

We determine $k_\perp$ using the WKB approximation $k_\perp$ through the relation

$$\nabla_\perp f \approx i k_\perp f \tag{34}$$

where f is as usual in the eikonal description

$$f = \tilde{f}e^{-in\left(\int \nu(r,\theta)d\theta - \phi\right)}. \tag{35}$$

Finally employing relation (26) yields

$$k_\perp = n\left(\nabla r\partial_r\tilde{q} + \nabla\theta\partial_\theta\tilde{q} - \nabla\phi\right). \tag{36}$$

The next step is to calculate $k_\perp \cdot \vec{v}_D$,

$$\begin{aligned}
\vec{k}_\perp \cdot e_\parallel \times \left(e_\parallel \cdot \nabla\right) e_\parallel &= \frac{J}{B^3}\left(\frac{B_\phi^3}{h_\phi^3}\left(g^{r\theta}\frac{q}{r}s\theta\Gamma^r_{\phi\phi} - g^{rr}\frac{q}{r}s\theta\Gamma^\theta_{\phi\phi}\right.\right.\\
&+ \left. g^{\theta\theta}q\Gamma^r_{\phi\phi} - g^{r\theta}q\Gamma^\theta_{\phi\phi}\right)\\
&+ \frac{B_\theta B_\phi^2}{h_\theta^2 h_\phi}\left(g^{r\theta}\frac{q}{r}s\theta\Gamma^r_{\theta\theta} - g^{rr}\frac{q}{r}s\theta\Gamma^\theta_{\theta\theta}\right.\\
&+ \left. g^{\theta\theta}q\Gamma^r_{\theta\theta} - g^{r\theta}q\Gamma^\theta_{\theta\theta}\right)\\
&- \frac{B_\theta B_\phi^2}{h_\theta h_\phi}\left(g^{rr}\frac{q}{r}s\theta\partial_\theta h_\theta^{-1} + g^{\phi\phi}\Gamma^r_{\phi\phi}\right.\\
&+ \left. g^{r\theta}q\partial_\theta h_\theta^{-1}\right)\\
&+ \frac{B_\theta^2 B_\phi}{h_\theta^2 h_\phi}\left(g^{r\theta}\frac{q}{r}s\theta\Gamma^r_{\theta\theta} - g^{rr}\frac{q}{r}s\theta\Gamma^\theta_{\theta\theta}\right.\\
&+ \left. g^{\theta\theta}q\Gamma^r_{\theta\theta} - g^{r\theta}q\Gamma^\theta_{\theta\theta}\right)\\
&+ \frac{B_\theta B_\phi}{h_\theta h_\phi}\left(g^{rr}\frac{q}{r}s\theta\Gamma^\phi_{\theta\phi}B_\theta h_\phi^{-1} - g^{rr}\frac{q}{r}s\theta\partial_\theta B_\theta h_\theta^{-1}\right.\\
&+ \left. g^{r\theta}q\Gamma^\phi_{\theta\phi}B_\theta h_\phi^{-1} - g^{r\theta}q\partial_\theta B_\theta h_\theta^{-1}\right)\\
&+ \frac{B_\theta^2}{h_\theta^2}\left(g^{rr}\frac{q}{r}s\theta\partial_\theta B_\phi h_\phi^{-1} - g^{r\theta}q\partial_\theta B_\phi h_\phi^{-1}\right.\\
&+ \left. \left. g^{\phi\phi}\Gamma^r_{\phi\phi}B_\phi h_\theta^{-1}\right)\right).
\end{aligned} \tag{37}$$

Now it is tedious but straight forward to calculate explicit expressions for $k_\parallel, k_\perp, \omega_D$. In the usual circular axisymmetric case these expressions become for $k_\perp, \omega_D$

$$\frac{\omega_D}{\omega_\star} \approx \epsilon_n\left(cos\theta + s\theta sin\theta\right) \tag{38}$$

$$k_\perp^2 \approx k_\theta^2\left(1 + s^2\theta^2\right) \tag{39}$$

The main advantage of using the analytical method is that it is easy to interpret the effects from different kinds of plasma cross sections on $k_\parallel, k_\perp, \omega_D$

(e.g. from elongation, Shafranov shift, triangularity etc). A second advantage is that it is easy to implement these effects into a an eigenvalue code.

IV Stellarators

Stellarators are 3D magnetic field configurations where the magnetic fields are generated by external coils. There is no need for a toroidal current in contrast to the tokamak configuration during operation. However, in experiments a toroidal current is often present for ohmic heating purposes. Stellarators may be the most flexible configuration from a physics point of view but there are often large forces on the external coils that act alternatingly inward and outward making extrapolations to higher fields and larger experiments unattractive. There are ways of constructing the windings to reduce this problem of large forces on the helical coils, however.

Most of the modern stellarators (e.g. Wendelstein 7-X [60], Quasi Poloidal Stellarator [61]) are optimized to minimize the neoclassical transport and therefore it is important to investigate the properties of anomalous transport in present stellarators. In the Quasi Poloidal hybrid Stellarator (QPS) experiment a confinement optimization is made for low plasma aspect ratio ($\bar{R}/\bar{a} \approx 2.6$) under the criterion of low neoclassical transport levels so that significant transport reduction is reached if enhanced confinement regimes are accessible.

The work presented in this thesis aims to extend the earlier work done on drift waves in simplified magnetic field configurations or with a simplified drift wave model [62] - [69]. There is some recent work done using the gyro kinetic model [70] - [72]. In Ref. [62] it was shown that in addition to the toroidally localized modes there are wells that may cause helical localization as well. In most of the recent papers [65] - [68] more general stellarator equilibria are used; however, simplified physical models are employed. The $i\delta$ model (non adiabatic electrons) artificially achieves a phase shift in the n and ϕ perturbations is employed. In specifying the instability mechanism (e.g. dissipative trapped electrons) an approximate model value of δ can be found. As for the tokamak, a ballooning mode structure is often assumed even in the stellarator case. This greatly simplifies the equations but may lead to problems. For low shear equilibria the distance between the resonant surfaces are large so that the coupling of the Fourier modes may be too weak; see Ref. [73] and a discussion thereof in Ref. [69] where it was reported that most of the important mode properties are found using the ballooning mode formalism in the $l = 2$ straight stellarator.

In this thesis only the flux coordinate system named Boozer-Grad [58],

[74] - [78] coordinates will be discussed. The Boozer-Grad coordinates are characterized by choosing the third Clebsch coordinate in a special way and the coordinate labels will be termed as (s, θ, ξ), where $s = 2\pi\psi/\psi_p$ is the normalized flux (radial) coordinate and θ, ξ are the generalized poloidal and toroidal angles, respectively. The magnetic field can be written in the form

$$\vec{B} = \frac{\dot{\psi}}{J}\left(e_\theta + q e_\xi\right) \tag{40}$$

where e_j and $\dot{\psi} = d\psi/ds$ are basis vectors and

$$J = \vec{e}_s \cdot \vec{e}_\theta \times \vec{e}_\xi = \frac{\bar{R}\dot{\psi}}{B^2}\left(B_\theta + q B_\xi\right). \tag{41}$$

In this coordinate system the geometry dependent terms can be written in the Ballooning representation as

$$\omega_{D_i} = \omega_{D_i}(s, \alpha, \xi) = \frac{B_0 \bar{R}}{B^2}\vec{k}_\perp \cdot \left(\vec{B} \times \left(\kappa + \nabla \ln B\right)\right) \tag{42}$$

$$\vec{k}_\perp = \vec{k}_\perp(s, \alpha, \xi; \theta_k) = \frac{\bar{a}}{q}\left(\nabla\xi - q\nabla\theta - \left(\frac{\xi - \xi_0}{q} - \theta_k\right)\frac{dq}{d\psi}\nabla\psi\right). \tag{43}$$

The last expressions can be approximated to Eqs 38 and 39 in Chapter III for a circular tokamak equilibrium.

In Ref. [64] it was reported that the radial localization width (and the micro turbulence level) in stellarators is to a large part influenced by the local magnetic shear and not the global magnetic shear as in the case for a tokamak, and thus the largest difference between tokamak configurations and stellarator configurations is that the local properties of the confining magnetic fields are significantly different. The local magnetic shear (s_L), the geodesic curvature (κ_G), the normal curvature (κ_N) and the variation of the magnetic field along the field line ($\vec{B}$) are important quantities when the drift wave stability is considered. When the tokamak configuration is studied most often the global magnetic shear (s) is treated which is the flux surface averaged local magnetic shear. It is possible to write the local magnetic shear as a linear combination of the global shear and a residual shear (s_R)

$$s_L = s + s_R \tag{44}$$

where the flux surface average of the residual shear vanishes. The normal and geodesic curvature are in Boozer coordinates

$$\kappa_N = \vec{\kappa} \cdot \frac{\nabla s}{|\nabla s|} \tag{45}$$

$$\kappa_G = \vec{\kappa} \cdot \left(\frac{\nabla s}{|\nabla s|} \times e_{\|} \right) \tag{46}$$

$$\vec{\kappa} = \left(e_{\|} \cdot \nabla \right) e_{\|} \tag{47}$$

where s is the normalized flux (radial) coordinate and $e_{\|}$ is a unit vector along the magnetic field. The regions of favorable and unfavorable curvature are determined by the signs of the normal and geodesic curvature, however, if the normal curvature is positive it is favorable. The effect of the geodesic curvature has to be determined from case to case.

V Zonal flows

The concept of zonal flow [79] - [81] is borrowed from geophysical fluid dynamics [82] - [83] where a flow in the direction of changing longitude within a given band of latitudes is called a zonal flow (it is constant in arbitrarily thin zones). Zonal flows in this work are low frequency, poloidally and azimuthally symmetric potential perturbations with small radial scale (i.e. $k_\theta = 0$, $k_\| = 0$ and $k_\perp$ finite). The zonal flows are essentially a limiting case of the more general notion of a "convective cell" [84] - [85]. It is instructive to show the difference in the $\vec{k}$ spectrum of zonal flows and ordinary turbulence.

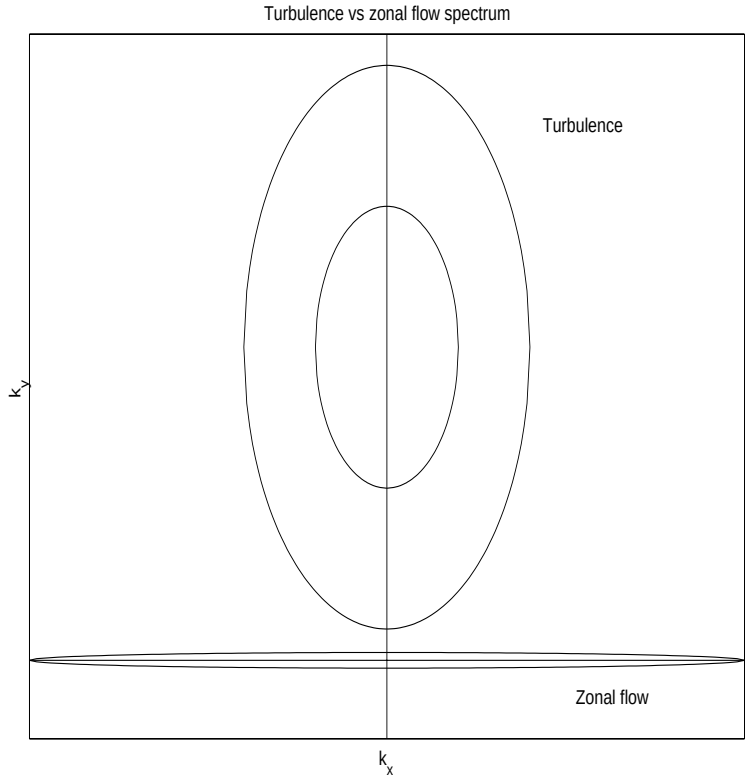

Figure: Turbulence versus zonal flow spectrum. The straight lines are $k_x = 0$ and $k_y = 0$ whereas the elliptical lines are contours of typical $\vec{k}$ spectrum values of turbulence and zonal flows, respectively.

Zonal flows are generated non-linearly by drift waves by the way of modulations in the radial flux of vorticity or the charge separation current. These flows are, effectively, sheared $\vec{E} \times \vec{B_0}$ flow layers which strain and distort the drift waves they co-exist with. There are a number of suggested damping mechanisms for zonal flows, two of the most important are the ion-ion collisions and the interference of Kelvin-Helmholtz instabilities that destroys zonal flows. The generation of zonal flows has recently been the subject of many scientific papers both analytically [86] - [94] and in computer simulations using gyrokinetic [95] - [97] and advanced fluid models [98] - [100] since they are expected to play an important role in the reduction of transport and turbulence found in in enhanced regimes of present fusion experiments [86], [95].

Unlike the drift waves ($k_\theta \neq 0$) which cause anomalous transport and are often considered having Boltzmann distributed electrons, the zonal flows ($k_\theta = 0$) have $\tilde{n}_e/n_0 \propto k_\perp^2 \rho_s^2 e\tilde{\phi}/T_e$. The proper electron density response is usually written as

$$\frac{\tilde{n}_e}{n_0} = \frac{e}{T_e}\left(\phi - \langle\phi\rangle\right) \tag{48}$$

where $\langle\phi\rangle$ is the flux surface average of ϕ. If this electron response is not used streamer like (radially elongated) structures form and grow indefinitely, and the turbulence never saturates [100].

It is found in recent non-linear collisionless gyrokinetic simulations that there is significant non-linear upshift (Dimits shift) in the effective critical gradient (R/L_{Ti}) needed for onset of turbulence. This upshift is caused by an undamped component of zonal flow [96] and may be reduced or removed by introducing collisionality that slowly damp the zonal flows [101]. In analytical estimations of zonal flow excitation a resonance is found close to marginal stability which is consistent with the non-linear simulations [94].

There are several methods for estimating the effects of zonal flows on turbulence analytically, among them are the wave kinetic approach [89], [102] - [106], the parametric instability method where a pump wave and sidebands generate the zonal flow [90], [93], [107] - [110] and the reductive perturbation method [94], [111] - [113]. To achieve a better understanding of these flows it is beneficial to proceed with a short instructive "calculation" closely following Ref. [105] where zonal flows appear in close connection with the wave kinetic approach. Consider a drift wave packet propagating radially in

an region of random zonal flow layers. Assume that that the zonal flows are, quasistationary, slowly varying in comparison with the drift waves ($\omega_{ZF} << \omega_{DW}$). When the drift wave packet meets the zonal flow layers the zonal flow will increase the drift wave $\langle k_r^2 \rangle$, since the zonal flows change the radial structure. Now, the drift wave frequency

$$\omega_{DW} \approx \frac{\omega_{\star e}}{1 + k_\perp^2 \rho_s^2} \tag{49}$$

will decrease and since the drift wave action density

$$N(k) = \frac{W(k)}{\omega_k} \tag{50}$$

is conserved (since we have assumed a quasi-stationarity case) the drift wave energy will decrease. The total energy of the drift wave and zonal flow system is conserved

$$W_{DW} + W_{ZF} = constant. \tag{51}$$

The zonal flow energy will increase which is suggestive of an instability and the initial perturbation will increase.

In the parametric instability method the fluctuations (electrostatic) are assumed to be coherent and composed of a single n ($n \neq 0$, toroidal mode number) drift wave ϕ_{DW} and a zonal flow mode ϕ_{ZF}. There are two sidebands ϕ_+ and ϕ_- produced by the modulation in the radial envelope due to ϕ_{ZF} with frequency ω_{ZF} and wavenumber k_{ZF}.

$$\phi_{DW} = \phi_0 + \phi_+ + \phi_- + c.c \tag{52}$$

Here c.c is the complex conjugate of the previous terms and ϕ_0 is the pump wave. This is a four wave coupling process with ϕ_0, ϕ_+, ϕ_- and ϕ_{ZF}, where ϕ_0 is considered to be linearly unstable whereas ϕ_+ and ϕ_- are considered linearly stable [90].

In the reductive perturbation method it is assumed that all fields may be expanded as a power series e.g.

$$f = \sum_p \epsilon^p f^p \tag{53}$$

$$f^p = \sum_l f_l^p(r, \xi, \tau) \exp il\left(k_\| z + k_\theta \theta - \omega t\right) \tag{54}$$

where the variables may be taken as $\xi = \epsilon\,(y - ut)$, u is the phase velocity and $\tau = \epsilon t^2$ where is a small parameter. This expansion is now inserted into the governing equations and then the equations are solved order by order. The linear dispersion relation is obtained to order ϵ, the group velocity to order ϵ^2 and zonal flow amplitude to order ϵ^3. The zonal flow ($l = o$) is obtained due to self interaction of the drift wave ($l = 1$). There is no need for the side bands in this case since the variation in ξ is slow.

In this thesis only the wave kinetic approach is employed.

VI Summary of papers

VI.1 Paper A

In Paper A the influence of the ion-temperature fluctuations on the the resistive ballooning mode stability in the strong ballooning limit is investigated. The model used to describe these modes is a two fluid model derived from the Braghinskii equations as a model for the electrons and an advanced fluid model for the ions. The derived eigenvalue equation is solved analytically assuming a specific form of the eigenmode, arriving at an algebraic dispersion relation. The algebraic dispersion relation is solved numerically using a standard root finding algorithm.

Comparison with earlier numerical simulations [42] shows that the analytical approach gives reasonable agreement for the mode growth. It is also shown that the ion-temperature fluctuations have a strong impact on the resistive mode. In particular, it is found that the mode is stabilized by FLR already at $\eta_i \geq 3$.

However, more work is needed to quantify and compare the FLR stabilization of the mode with the stabilization due to sheared rotation.

VI.2 Paper B

The work in paper B is based on an advanced fluid model for the ions as in Paper A whereas the electrons are assumed to be Boltzmann distributed. The ion-temperature-gradient (ITG) driven mode stability properties are studied in a generalized $s - \alpha$ model that allows for non-circular cross section. An eigenvalue equation is derived and is solved numerically using a standard shooting technique. In particular, the paper investigates the effects of elongation (κ) and Shafranov shift on the ITG mode. Approximate results are also calculated in the strong ballooning limit.

The effects of non-circular cross section enter mainly in the magnetic drift frequency; however, the FLR parameter and the parallel wavenumber are also modified. The effect of elongation is two-fold: (1) it is stabilizing for small ϵ_n and (2) it is destabilizing in a region of parameter space with large ϵ_n. However, for sufficiently large elongation a stabilization is eventually found. The influence of Shafranov shift is rather weak but tends to be stabilizing.

In addition, the spectrum of the unstable modes is shifted towards shorter

wavelengths for elongated equilibria. This shift tends to reduce the transport by reducing the correlation length in the plasma. The present paper indicates that for realistic tokamak parameters the model predicts a slight destabilization of the η_i-mode in the core where the density profiles are flat whereas in the edge where the density profiles are peaked we expect a stabilization. To characterize the total effects of elongation on the confinement time a more elaborate transport code study is needed which treats the core and edge transport processes self-consistently and which includes the effects of non-circular cross sections.

VI.3 Paper C

In paper C the resistive edge modes (collisional η_i-modes and resistive ballooning modes (RBM)) are investigated in non-circular tokamak equilibria, using the same physical model as in Paper A but the eigenvalue problem is solved numerically. The geometrical effects enter in the magnetic drift frequency (ω_D) and in the perpendicular ($k_\perp$) and the parallel ($k_\parallel$) length scales. Paper C is divided into two parts; the first part treats the collisional η_i-mode while the second part treats the RBM.

In the first part it is found that the η_i-mode may be either stabilizing or destabilizing by the electron-ion collisions depending on the parameters used. It is found that the scaling of elongation is similar to that obtained for the collisionless η_i-mode studied in paper B.

In part two the RBM is investigated and the stabilization of the RBM with η_i as seen in Paper A is recovered and may be enhanced by increasing elongation. For edge parameters (i.e. ϵ_n small) a favorable scaling with elongation is expected as seen in Fig. 6.

The maximum growth rate of the RBM and the collisional η_i-modes are of equal magnitude with $k_\theta\rho \approx 0.15$ for maximum growth rate of the RBM and $k_\theta\rho \approx 0.3$ for the collisional η_i-modes.

In conclusion, the elongation scaling of the η_i- and ballooning modes seem to be more favorable at the edge, where ϵ_n is small, than in the core. As suggested by recent transport code simulations, the scaling originating from the edge may be more important for determining the total effects of plasma elongation on the energy confinement time.

VI.4 Paper D

The reactive ITG driven mode stability in an H-1NF stellarator equilibrium is calculated in paper D. The physical model used is the same model as in paper B. VMEC is employed to calculate the stellarator equilibria and the output is tranformed into the Boozer coordinate basis which is used for all calculations. Results of numerical calculations have been presented on a field line of reference passing through $\theta = \xi = 0$ on the magnetic surface $s = 0.4$. All the results are compared to the corresponding tokamak results reported earlier in [36]. The main concern of this paper is to make a first attempt to calculate the ITG mode stability for a stellarator equilibrium using the ballooning mode formalism; however, no attempt is made to cover the vast parameter range resulting from the various operational modes.

The critical temperature gradient needed to obtain instability is $\eta_i \approx 2.2$ which is slightly larger than the threshold found for the corresponding tokamak; this may be due to the negative magnetic shear in the stellarator. The effect of small and large temperature ratios is found to be stabilizing on the modes. The parameter θ_k controls the magnitude of $\vec{k}_\perp$ along the outward normal to the flux surface. A slow variation of the growth rate and real frequency is found when the parameter θ_k is varied at the magnetic surface $s = 0.4$. This is found to be due to the small "global" magnetic shear ($\dot{q}/q = -0.027$) whereas at the $s = 0.9$ magnetic surface the shear is significantly larger ($\dot{q}/q = -0.11$) and the variation with θ_k is larger.

VI.5 Paper E

A comparison of the ITG mode instability for three different cases namely, the H-1NF stellarator, a numerical circular 3d tokamak and the analytical $s-\alpha$ equilibria is done in paper E. The physical model employed is the same as in paper B. The numerical equilibria utilized are calculated with VMEC and the output is transformed into the Boozer coordinate basis. Growth rates and real frequencies are compared for the most localized mode which also corresponds to the largest growth rate.

Good agreement is found between the numerical tokamak equilibrium and the $s-\alpha$ model equilibrium for small and intermediate radial positions. The growth rates for the stellarator and the tokamak are comparable whereas the modulus of the real frequency for the stellarator is significantly larger than

the tokamak result and this is partly explained by the stronger curvature of the stellarator. The η_i threshold value is slightly increased and a stronger stabilization of the modes is found for large ϵ_n (compression) in the stellarator case which may be caused by the negative magnetic shear in the stellarator. This is due to the fact that the negative magnetic shear in the stellarator tends to decrease the curvature and thus the growth rate decreases. This is displayed using the corresponding result for the analytical model with reversed shear.

The differences in the results obtained for the stellarator and the tokamak and the variation with the radial coordinate can all be understood in terms of the changing curvature.

VI.6 Paper F

In this work the zonal flow growth rate in toroidal ion-temperature-gradient (ITG) mode turbulence including the effects of elongation is studied analytically. The scaling of the zonal flow growth with plasma parameters is examined for typical tokamak parameter values. The physical model used for the toroidal ITG driven mode is based on the ion continuity and ion temperature equations whereas the zonal flow evolution is described by the vorticity equation. The present model is electrostatic and FLR effects and electron trapping are neglected. The time evolution of the adiabatic invariant in toroidal ITG turbulence is described by the wave-kinetic equation which gives the coupling between the zonal flow and toroidal ITG mode perturbations. An algebraic equation is derived describing the zonal flow excitation retaining effects of elongated plasma cross sections which is solved numerically.

A resonance in the zonal flow excitation level is found close to marginal stability, consistent with the non-linear simulation results of the Cyclone work [105]. For peaked density profiles (small $\epsilon_n = 2L_n/L_B$), a strong excitation of zonal flows with γ/γ_{ITG} is found which is substantially increased with elongation whereas for most other cases the effects of elongation are weak. Moreover, the zonal flow excitation grows linearly with the wavenumber for zero collisional damping whereas for non-zero damping the zonal flow excitation is significantly reduced.

VII Acknowledgments

First of all, I would like to thank my supervisors Dr. Hans Nordman and Professor Jan Weiland for their support and advice. I would also like to thank Dr. Hans-Georg Gustavsson for his help with all problems concerning the computers and proofreading. I am also grateful to the other members of the Department of Electromagnetics for many enlightening discussions during lunch and coffee breaks. Last but not least, I am in debt to my parents for their encouragement and support and above all to Melissa Renov for her love and endurance. You are the best.

Göteborg April 2002
Johan Anderson

References

[1] J. P. Freidberg, Rev. Mod. Phys. **54**, 801 (1982)

[2] P. C. Liewer, Nucl. Fusion **25**, 543 (1985)

[3] F. Wagner, U. Stroth, Plasma Phys. Contr. Fusion **35**, 1321 (1993)

[4] A. A. Galeev, R. Z. Sagdeev, Sov. Phys. JETP **26**, 752 (1968)

[5] F. L. Hinton, R. D Hazeltine, Rev. Mod. Phys. **48**, 239 (1976)

[6] S. P. Hirschman, D. J. Sigmar, Nucl. Fusion **21**, 1079 (1981)

[7] R. J. Bickerton, Plasma Phys. Contr. Fusion **39**, 339 (1997)

[8] T. H. Dupree, Phys. Fluids **10**, 1059 (1967)

[9] J. Weiland, H. Nordman, "Theory of Fusion Plasmas", Proc. Varenna-Lausanne Int. Workshop, Chexbres, Switzerland (1988)

[10] H. Nordman and J. Weiland, Nucl. Fusion **29**, 251 (1989)

[11] H. Nordman, J. Weiland and A. Jarmén, Nucl. Fusion **30**, 983 (1990)

[12] W. Horton et al., Phys. Fluids **31**, 2971 (1988)

[13] A. Zagorodny, J. Weiland, Phys. Plasmas **6**, 2359 (1999)

[14] F. Levington et al., Phys. Rev. Lett. **75**, 4417 (1995)

[15] E. A. Lazarus et al., Phys. Rev. Lett. **77**, 2714 (1996)

[16] J. Hugill, Plasma Transport 35th Culham Plasma Physics Summer School

[17] E. Strait, Phys. Rev. Lett. **75**, 4221 (1995)

[18] JET Team, (Proc. 16th Int. Conf. Montreal 1996) Vol. 1 IAEA, Vienna (1997)

[19] F. Wagner et al., Phys. Rev. Lett. **49**, 1408 (1982)

[20] J. Weiland and H. Nordman, Nucl. Fusion **31**, 390 (1991)

[21] M. Fröjdh, P. Strand, J. Weiland and J. P. Christiansen, Plasma Phys. Contr. Fusion **38**, 325 (1996)

[22] P. Strand, H. Nordman, J. Weiland and J. P. Christiansen, Nucl. Fusion **38**, 545 (1998)

[23] J. Weiland and H. Nordman, Phys. Fluids B **5**, 1669 (1993)

[24] P. Strand, H. Nordman, J. Weiland and J. P. Christiansen, Plasma Phys. Contr. Fusion **41**, 1441 (1999)

[25] H. Nordman, P. Strand, J. Weiland and J.P. Christiansen, Nucl. Fusion **39**, 1157 (1999)

[26] L. I. Rudakov, R.Z. Sagdeev, Sov. Phys. Dokl. **6**, 415, (1961)

[27] O. P. Pogutse, Sov. Phys. JETP **25**, 498 (1967)

[28] W. Horton, D. I. Choi, W. M. Tang, Phys. Fluids **24**, 1077 (1981)

[29] P. N. Guzdar, L. Chen, W. M. Tang et al., Phys. Fluids **26**, 673 (1983)

[30] G. A. Hallock, A. J. Wootton, R. V. Bravence et al., Bull. Am. Phys. Soc. **34**, 2152 (1989)

[31] B. Coppi, M.N. Rosenbluth, R.Z. Sagdeev, Phys. Fluids **10**, 582 (1967)

[32] B. Coppi, F. Pegoraro, Nucl. Fusion **17**, 969 (1977)

[33] P. N. Guzdar, L. Chen, W. M. Tang, P. H. Rutherford, Phys. Fluids **26**, 673 (1983)

[34] A. Jarmén, P. Andersson, J. Weiland, Nucl. Fusion **27**, 941 (1987)

[35] J. Nilsson, M. Liljeström, J. Weiland, Phys. Fluids B **2**, 2568 (1990)

[36] S. C. Guo, J. Weiland, Nucl. Fusion **37**, 1095 (1997)

[37] J. Weiland, "Collective Modes in Inhomogeneous Plasmas, Kinetic and Advanced Fluid Theory", IOP Publishing Bristol (2000)

[38] D. R. McCarthy, P. N. Guzdar, J. F. Drake et al., Phys. Fluids B **4**, 1846 (1992)

[39] A. J. Wooton, B. A. Carreras, H. Matsumoto et al., Phys. Fluids B **2**, 2879 (1990)

[40] P. N. Guzdar, J. F. Drake, D. R. McCarthy et al., Phys. Plasmas **5**, 3712 (1993)

[41] B. D. Scott, Plasma Phys. Contr. Fusion **39**, 1635 (1997)

[42] S. V. Novakovskii, P. N. Guzdar, J. F. Drake et al., Phys. Plasmas **2**, 781 (1995)

[43] J. W. Connor, R. J. Hastie, J. B. Taylor, Proc. R. Soc. London Ser. A 365, 1 (1979)

[44] R. L. Dewar, A. H. Glasser, Phys. Fluids **26**, 3038 (1983)

[45] R. D. Hazeltine, J. D. Meiss, Plasma Confinement, Frontiers in Physics (1992)

[46] C. Mercier, N. Luc, Report No. EUR-5127e 140 (1974)

[47] J. W. Connor, R. J. Hastie, J. B. Taylor, Phys. Rev. Lett. **40**, 396 (1978)

[48] J. M. Greene, M. S. Chance, Nucl. Fusion **21**, 453 (1981)

[49] R. L. Miller, M. S. Chu, J. M. Greene et al., Phys. Plasmas **5**, 973 (1998)

[50] A. J. Redd, A. H. Kritz, G. Bateman et al., Phys. Plasmas **4**, 1162 (1999)

[51] P. N. Yshmanov et. al., Nucl. Fusion **30**, 1999 (1990)

[52] T. C. Luce, C.C. Petty, J. E. Kinsey, 28th EPS Conference on Controlled Fusion and Plasma Physics Madeira, Portugal, 2001

[53] D. D. Hua, Y. Q. Yu, T. K. Fowler, Phys. Fluids **34**, 3216 (1992)

[54] J. Kesner, Nucl. Fusion **31**, 511 (1991)

[55] R. E. Waltz, R. L. Miller, Phys. Plasmas **6**, 4265 (1999)

[56] G. Rewoldt, W.M. Tang, M.S. Chance, Phys. Fluids **25**, 480 (1982)

[57] K. R. Chu, E. Ott, W. M. Manheimer, Phys. Fluids **21**, 664 (1978)

[58] W. D. D'haeseleer, W. N. G. Hitchon, J. D. Callen, "Flux Coordinates and Magnetic Field Structure", Springer-Verlag (1991)

[59] M. Nakahara, "Geometry, Topology and Physics", IOP Publishing (1990)

[60] G. Grieder, C. D. Biedler, H. Massberg et al., Plasma Phys. Contr. Nucl. Fusion Research (IAEA) **3**, 525 (1990)

[61] D. A. Spong, S. P. Hirschman et al., Nucl. Fusion **41** 711 (2001)

[62] A. Bhattacharjee, J. E. Sedlak, P. L. Simillion et al., Phys. Fluids **26**, 880 (1983)

[63] N. Dominguez, B. A. Carreras, V. E. Lynch et al. Phys., Fluids B **4**, 2894 (1992)

[64] R. Waltz, A. H. Boozer Phys. Fluids B **5**, 2201 (1993)

[65] M. Persson, J. L. V. Lewandowski, H. Nordman, Phys. Plasmas **3**, 3720 (1996)

[66] M. Persson, J. L. V. Lewandowski, Plasma Phys. Contr. Fusion **39**, 1941 (1997)

[67] J. L. V. Lewandowski, Phys. Plasmas **4**, 4023 (1997)

[68] M. Persson, M. Nadeem, J. L. V. Lewandowski, Plasma Phys. Contr. Fusion **42**, 203 (2000)

[69] R. Kleiber, Phys. Plasmas **8**, 4090 (2001)

[70] T. Kuroda, H. Sugama, R Kanno et al., J. Plasma and Fusion Research SERIES **2**, 105 (1999)

[71] G. Rewoldt, L-P Ku, W. M. Tang et al., Phys . Plasmas **6**, 4705 (1999)

[72] T. Kuroda, H. Sugama, R Kanno et al., J. Phys. Soc. Japan **69**, 2485 (2000)

[73] J. W. Connor, J. B. Taylor, Phys. Fluids **30**, 3180 (1987)

[74] H. Grad, Plasma Phys. Contr. Nucl. Fusion Research (IAEA) **3**229 (1971)

[75] A. H. Boozer, Phys. Fluids **23**, 904 (1980)

[76] A. H. Boozer, Phys. Fluids **24**, 1999 (1981)

[77] P. J. Catto, R. D. Hazeltine, Phys. Fluids **24**, 1663 (1981)

[78] O. Betancourt, P. Garabedian, Phys. Fluids **28**, 912 (1985)

[79] A. Hasegawa, M. Wakatani, Phys. Rev. Lett. **59**, 1581 (1987)

[80] G. W. Hammett, M. A. Beer, W. Dorland et al., Plasma Phys. Contr. Fusion **35**, 973 (1993)

[81] V. B. Lebedev, P. H. Diamond, V. D. Shapiro et al., Phys. Plasmas **2**, 4420 (1995)

[82] F. H. Busse, Chaos **4**, 123 (1994)

[83] P. B. Rhines, Chaos **4**, 315 (1994)

[84] A. Hasegawa, C. G. Maclennan, Y. Kodama, Phys. Fluids **22**, 2122 (1979)

[85] R. Z. Sagdeev, V. D. Shapiro, V. I. Shevchenko, Sov. J. Plasma Phys. **4**, 551 (1978)

[86] H. Biglari, P.H. Diamond and P.W. Terry, Phys. Fluids B **2**, 1 (1990)

[87] P. H. Diamond and Y. B. Kim, Phys. Fluids B, **5** 2343 (1991)

[88] A. I. Smolyakov et al, Phys. Rev. Lett. B **3**, 1626 (1999)

[89] A. I. Smolyakov, P. H. Diamond, M. V. Medvedev, Phys. Plasmas, **7** 3987 (2000)

[90] L. Chen, Z. Lin and R. White, Phys. Plasmas **7**, 3129 (2000)

[91] A. I. Smolyakov et al, Phys. Rev. Lett. B **4**, 491 (2000)

[92] M. A. Melkov, P.H. Diamond and A.I. Smolyakov, Phys. Plasmas **8**, 1553 (2001)

[93] P. N. Guzdar, R. G. Kleva and L. Chen, Phys. Plasmas **8**, 459 (2001)

[94] S. Mahajan, J. Weiland, Plasma Phys. Contr. Fusion **42**, 987 (2000)

[95] Z. Lin, T. S Hahm, W. W. Lee, W. M. Tang and R. B. White, Science 281, 1835 (1998)

[96] Z. Lin, T. S Hahm, W. W. Lee, W. M. Tang and P. H. Diamond, Phys. Rev. Lett. **83**, 3645 (1999)

[97] A. Dimits, T. J. Williams, J. A. Byers and B. I. Cohen, Phys. Rev. Lett. **77** 71 (1996)

[98] G. Hammet, M. Beer, W. Dorland, S. C. Cowley and S.A. Smith, Plasma Phys. Contr. Fusion **35**, 937 (1993)

[99] R. E. Waltz, G. D. Kerbel and A. J. Milovich, Phys. Plasmas **1**, 2229 (1994)

[100] A. Dimits, G. Bateman, M. A. Beer et al., Phys. Plasmas **7**, 969 (2000)

[101] Z. Lin, T. S Hahm, W. W. Lee, W. M. Tang and R. B. White, Phys. Plasmas **7**, 1857 (2000)

[102] A. A. Vedenov, A. V. Gordeev, L. I. Rudakov, Plasma Phys. **9**, 719 (1967)

[103] P. H. Diamond, M. N. Rosenbluth, F. L. Hinton, M. Malkov et al., Plasma Phys. Nucl. Fusion Research (IAEA 1998) p. IAEA-CN-69/TH3/1

[104] A. I. Smolyakov, P. H. Diamond, Phys. Plasmas, **6** 4410 (1999)

[105] P. H. Diamond, S. Champeaux, M. Malkov et al., Nucl. Fusion **41**, 1067 (2001)

[106] J. A. Krommes, C-B. Kim, Phys. Rev. E **62**, 8508 (2000)

[107] J. Drake, J. Finn, P. N. Guzdar, Phys. Fluids B **4**, 488 (1992)

[108] J. Finn, J. Drake, P. N. Guzdar, Phys. Fluids B **4**, 2758 (1992)

[109] P. N. Guzdar, Phys. Plasmas **2**, 4174 (1995)

[110] P. N. Guzdar, R. G. Kleva, A. Das ,Phys. Plasmas **8**, 3907 (2001)

[111] K. Nozaki, T. Taniuti, K. Watanabe J. Phys. Soc. Japan **46**, 983 (1979)

[112] K. Nozaki, T. Taniuti, K. Watanabe J. Phys. Soc. Japan **46**, 991 (1979)

[113] J. Weiland, H. Sanuki, C. S. Liu, Phys. Fluids **24**, 93 (1981)